

Positivity Preserving Density Matrix Minimization at Finite Temperatures via Square Root

Jacob Leamer,¹ William Dawson,² and Denys I. Bondar¹

¹*Department of Physics and Engineering Physics, Tulane University, 6823 St. Charles Ave., New Orleans, LA 70118, USA*

²*RIKEN Center for Computational Science, Kobe, Hyogo, 650-0047, Japan.*

(Dated: 8 December 2023)

We present a Wave Operator Minimization (WOM) method for calculating the Fermi-Dirac density matrix for electronic structure problems at finite temperature while preserving physicality by construction using the wave operator, i.e., the square root of the density matrix. WOM models cooling a state initially at infinite temperature down to the desired finite temperature. We consider both the grand canonical (constant chemical potential) and canonical (constant number of electrons) ensembles. Additionally, we show that the number of steps required for convergence is independent of the number of atoms in the system. We hope that the discussion and results presented in this article reinvigorates interest in density matrix minimization methods.

I. INTRODUCTION

The ability to determine the electronic structure is of critical importance for obtaining a proper understanding of the quantum behavior of materials. One way of many¹ to achieve this is by computing the finite temperature, effective single-electron density matrix $\hat{\rho}$ (or Gibbs state) that statistically describes the system state in question

$$\hat{\rho}(\beta) = \frac{\hat{I}}{\hat{I} + \exp[\beta(\hat{H} - \mu)]}, \quad (1)$$

where \hat{H} is the N -dimensional Hamiltonian operator, \hat{I} the identity operator, and $\beta = 1/(kT)$ is the inverse temperature of the system. Once $\hat{\rho}$ has been determined, it can be used to obtain other information about the system such as the number of electrons $N_e = \text{Tr}(\hat{\rho})$ or the electronic energy $E = \text{Tr}(\hat{H}\hat{\rho})$, which in general depends upon $\hat{\rho}$. These quantities can then be used to obtain other observables of interest like the specific heat $C_v = \frac{dE}{dT}$ where T is the temperature of the system.

Unfortunately, conventional methods for obtaining $\hat{\rho}$ are known to scale poorly with the size of the system in question. This is because they generally rely on diagonalization of \hat{H} or the multiplication of dense matrices, both of which scale as $O(N^3)$. As such, a lot of effort has been directed toward the development of new methods for solving these problems that scale linearly with $N^{2,3}$. These methods have proven useful in performing Density Functional Theory calculations^{4,5}, including *ab initio* molecular dynamics⁶⁻⁹; this success has prompted the general development of a number of open-source libraries¹⁰⁻¹⁷.

Despite their usefulness, the vast majority of the linear-scaling methods are focused on obtaining the density matrix describing zero-temperature states, i.e., the ground state of the system. However, in recent years there has been a great deal of interest in the development of methods for calculating $\hat{\rho}$ at finite temperature^{16,18-24}, including stochastic methods^{25,26}. Density Functional Theory calculations at finite temperature²⁷⁻²⁹ are a re-

quirement for the study of warm dense matter³⁰, may be used to describe static correlation³¹⁻³³, can accelerate convergence of self-consistent field methods³⁴, or be employed for studying chemical reactions²³. To contribute to this growing body of work, we present methods for calculating $\hat{\rho}$ at a finite temperature for electronic systems that are in the grand canonical or canonical ensembles.

Our methods are based on the *Wave Operator Minimization* (WOM), where the wave operator refers to the square root of the density matrix. The core idea of this method is that the square root of the Fermi-Dirac state is the solution to an initial value problem. This is conceptually similar to the approach utilized in density matrix minimization methods (DMM)³⁵⁻⁵⁰, but casting the initial value problems in terms of the square root of $\hat{\rho}$ yields solutions that are manifestly positive and Hermitian – two crucial physicality constraints.

The formalism of the square root of a density matrix – also known as the wave operator – has been used for foundational research⁵¹⁻⁵⁹. The wave operator also has turned out to be as an efficient computational tool for both Markovian and non-Markovian open quantum system dynamics⁶⁰. To best of our knowledge, the current paper would perhaps be the first deployment of the density matrix square root for electron structure calculations. Note that the square root of the electronic density, which is contained in the diagonal elements of a density matrix, has been used as a numerical tool for orbital free density functional theory⁶¹⁻⁶³.

The rest of the paper is organized as follows. In Sec. II, we introduce the WOM method using the Gibbs state and contrast it with a DMM-like approach. Sections III and IV discuss the application of WOM to fermionic systems that obey the statistics of the grand canonical and canonical ensembles, respectively. We discuss the algorithmic implementation of our methods and demonstrate its effectiveness by considering a models of bulk aluminum and silicon of different system sizes in Sec. V.

II. FROM FINITE TEMPERATURE DMM TO WOM

As mentioned previously, the difficulty with calculating $\hat{\rho}$ is that the computational costs typically scale as $O(N^3)$, which makes it infeasible for many systems of interest. Approaches that are based on minimization, however, are able to achieve $O(N)$ scaling by using sparse matrix algebra computational kernels. Fortunately, sparsity naturally arises in electronic structure calculations from Kohn's nearsightedness principle^{64,65}, which holds even for metals at finite temperatures. Because of this, minimization-based approaches are a natural consideration for the development of new methods for solving electronic structure problems.

We were further motivated to consider an iterative approach for calculating $\hat{\rho}$ at finite temperatures by the method developed by Bloch⁶⁶ to obtain the Gibbs state. For such states

$$\frac{d\hat{\rho}}{d\beta} = -\hat{H}\hat{\rho}. \quad (2)$$

This equation along with the initial condition $\hat{\rho}(0) = \hat{I}$ (i.e. the identity matrix) can be used to construct an iterative method for finding $\hat{\rho}$ at any given temperature. The problem with using Eq. (2) is that numerical errors in the calculation may make $\hat{\rho}$ non-Hermitian. To avoid this issue, Bloch symmetrized Eq. (2) in the following manner

$$\frac{d\hat{\rho}}{d\beta} = -\frac{\hat{H}\hat{\rho}}{2} - \frac{\hat{\rho}\hat{H}}{2}. \quad (3)$$

To elucidate the power of the Bloch method, let us prove that evolving $\hat{\rho}$ via Eq. (3) preserves not only Hermiticity but also the positivity of the density matrix. The representation of Eq. (3) via a finite difference approximation

$$\frac{\hat{\rho}(\beta + \delta\beta) - \hat{\rho}(\beta)}{\delta\beta} = -\frac{\hat{H}\hat{\rho}(\beta)}{2} - \frac{\hat{\rho}(\beta)\hat{H}}{2} + O(\delta\beta), \quad (4)$$

where $\delta\beta$ is a small inverse temperature increment, can be recast as

$$\hat{\rho}_{n+1} = \left(\hat{I} - \frac{\delta\beta}{2} \hat{H} \right) \hat{\rho}_n \left(\hat{I} - \frac{\delta\beta}{2} \hat{H} \right)^\dagger + O(\delta\beta^2). \quad (5)$$

Here, $\hat{\rho}_n = \hat{\rho}(\beta)$ and $\hat{\rho}_{n+1} = \hat{\rho}(\beta + \delta\beta)$. Because the r.h.s. of Eq. (5) is in the form $A\hat{\rho}_n A^\dagger$, we know that this method also preserves the positivity of $\hat{\rho}$ ⁶⁷. As such, we can think of this iterative method as behaving like a quantum channel modeling cooling that maps $\hat{\rho}_n$ from a higher temperature state to a lower one, $\hat{\rho}_{n+1}$. This approach is conceptually similar to the quenching approach utilized for the Fermi operator expansion method by Aarons and coworkers²⁴. One key difference, however, is that the quenching Fermi operator approach does not explicitly preserve the positivity of $\hat{\rho}$, while the symmetrized derivative approach in Eq. (3) can be shown to preserve positivity.

Whereas the symmetrization approach generalizes to the Fermi-Dirac state, we found that it is easier to perform the calculations in terms of WOM. Let us introduce our method by evaluating the Gibbs state $\hat{\rho}(\beta)$. The key idea is to represent the density matrix as

$$\begin{aligned} \hat{\rho}(\beta) &= \hat{\Omega}(\beta)^\dagger \hat{\Omega}(\beta), \\ \hat{\Omega}(\beta) &= \exp(-\beta \hat{H}/2), \end{aligned} \quad (6)$$

where the square root of the Gibbs state $\hat{\Omega}(\beta)$ is the solution to the initial value problem

$$\frac{d}{d\beta} \hat{\Omega}(\beta) = -\frac{1}{2} \hat{H} \hat{\Omega}(\beta), \quad \hat{\Omega}(0) = \hat{I}. \quad (7)$$

The main advantage of the WOM method is that one can use *any* numerical method for solving Eq. (7) and the resulting Gibbs state (6) is manifestly positive. That is we are not restricted to specific finite difference methods, e.g., Eq. (5).

III. WOM FOR THE GRAND CANONICAL ENSEMBLE

In this section, we apply WOM to fermionic systems that are described by the Fermi-Dirac distribution in a non-orthonormal basis and whose statistical behavior is described by the grand canonical ensemble in which systems are allowed to exchange both energy and electrons with their environment. For us, this means that we need to fix the value of the chemical potential μ before applying our method, which will allow the number of electrons N_e to change.

Because we wish to consider a non-orthonormal basis, we need to introduce the overlap matrix S . The overlap matrix is a square, positive-definite matrix that characterizes the overlap between the basis vectors used to describe a system. For basis vectors $|i\rangle, |j\rangle$ the elements of the overlap matrix are given by the following expression

$$S_{ij} = \langle i|j\rangle. \quad (8)$$

We use P and H to denote the matrix representations of $\hat{\rho}$ and \hat{H} respectively in the non-orthonormal basis. The elements of these matrices P and H are

$$P_{ij} = \langle i|\hat{\rho}|j\rangle, \quad H_{ij} = \langle i|\hat{H}|j\rangle. \quad (9)$$

Using these representations, we can obtain the following expression for the Fermi-Dirac distribution in a general basis (see Appendix A for details)

$$P(\beta) = S [I + \exp[\beta(S^{-1}H - \mu I)]]^{-1}. \quad (10)$$

The corresponding WOM representation is

$$\begin{aligned} P(\beta) &= \Omega(\beta)^\dagger \Omega(\beta), \\ \Omega(\beta) &= S^{1/2} [I + \exp[\beta(S^{-1}H - \mu I)]]^{-1/2}, \end{aligned} \quad (11)$$

(see Appendix B for proof) and the initial value problem to which $\Omega(\beta)$ is the solution is

$$\frac{d\Omega}{d\beta} = -\frac{1}{2}\Omega \left[I - (S^{-1/2}\Omega)^2 \right] (S^{-1}H - \mu I), \quad (12)$$

$$\Omega(0) = \sqrt{\frac{S}{2}}. \quad (13)$$

Several DMM methods have been developed for handling systems in a non-orthogonal basis and with statistics described by the grand canonical ensemble^{49,50}. However, these methods are aimed at obtaining the ground state density matrix and thus rely heavily upon the McWeeny purification algorithm⁶⁸ to enforce idempotency and positivity on the resulting P . Unlike the approaches used in many DMM methods^{35–37,49,50,69}, Eq. (11) is shown to be explicitly positivity-preserving without the need for something like the McWeeny purification algorithm or an exponential parameterization^{45–48}.

IV. WOM FOR THE CANONICAL ENSEMBLE

It is also possible to apply WOM to systems described by the canonical ensemble in which a system is only allowed to exchange energy with the environment. This means that N_e should remain constant as we iterate towards the desired temperature. Note that in the non-orthogonal basis, $N_e = \text{Tr}[S^{-1}P]$. This constraint can be enforced by updating the value of μ with every step. Thus, we now have $\mu = \mu(\beta)$ and Eq. (10) becomes

$$P(\beta) = S \left[I + \exp[\beta(S^{-1}H - \mu(\beta)I)] \right]^{-1}. \quad (14)$$

The corresponding form of Ω is

$$\Omega(\beta) = S^{1/2} \left[I + \exp[\beta(S^{-1}H - \mu(\beta)I)] \right]^{-1/2}. \quad (15)$$

For brevity, we introduce

$$X = \Omega \left[I - (S^{-1/2}\Omega)^2 \right], \quad (16)$$

$$A = S^{-1}H. \quad (17)$$

Now the derivative with respect to β is

$$\frac{d\Omega}{d\beta} = -\frac{1}{2}X \left(A - \mu - \beta \frac{d\mu}{d\beta} \right). \quad (18)$$

To guarantee that N_e is conserved while β is increasing, we solve $\frac{dN_e}{d\beta} = \frac{d}{d\beta} \text{Tr}[S^{-1}\Omega(\beta)^\dagger\Omega(\beta)] = 0$ for the unknown $\mu + \beta \frac{d\mu}{d\beta}$ to obtain

$$\mu + \beta \frac{d\mu}{d\beta} = \frac{\text{Tr}[AS^{-1}X^\dagger\Omega + \Omega^\dagger XS^{-1}A^\dagger]}{\text{Tr}[S^{-1}X^\dagger\Omega + \Omega^\dagger XS^{-1}]}. \quad (19)$$

Then we substitute Eq. (19) into Eq. (18) to construct the sought initial value problem

$$\frac{d\Omega}{d\beta} = -\frac{1}{2}X \left(A - \frac{\text{Tr}[AS^{-1}X^\dagger\Omega + h.c.]}{\text{Tr}[S^{-1}X^\dagger\Omega + h.c.]} \right), \quad (20)$$

$$\Omega(0) = \sqrt{\frac{N_e}{N}} \sqrt{\frac{S}{2}}, \quad (21)$$

where Eq. (21) has been constructed so that $\text{Tr}[S^{-1}P(0)] = N_e$. By solving this initial value problem, we can calculate $P(\beta) = \Omega(\beta)^\dagger\Omega(\beta)$ while ensuring that N_e is conserved.

A review of DMM methods reveals that the presence of $\frac{d\mu}{d\beta}$ in Eq. (18) appears to be an often overlooked subtlety. The methods that explicitly preserve N_e ^{35,69} make no mention of the importance of updating the value of μ , while others^{36,37,49,50} focus on the grand canonical ensemble and only refer to the fact that conserving μ is easier than conserving N_e . One method⁷⁰ that does mention the importance of updating μ does so by solving a third order polynomial as a part of a two-stage steepest descent algorithm. In contrast, our approach of updating μ only requires evaluating the traces of matrices and taking their ratio. It is also worth noting again that WOM preserves positivity explicitly without the need for the McWeeny purification algorithm used in the DMM methods.

The calculation of μ is another key difference between our minimization approach and the quenching Fermi operator expansion approach²⁴. In the latter, μ is calculated using a root-finding approach that requires the inversion of matrices. In contrast, our approach updates the value of μ to preserve N_e while iterating P to the desired temperature.

V. ILLUSTRATIONS

To illustrate WOM, we first consider a tight-binding model of aluminum. The tight-binding model⁷¹ has been used to great success in a number of solid state applications^{72,73} and thus serves as a useful benchmark for developing methods of solving electronic structure problems. Aluminum is a simple metal that has been studied extensively^{74,75}, which makes it convenient to obtain Hamiltonians for a variety of system sizes. This in turn allows us to test the scaling of the adaptive step implementations of our methods while testing their effectiveness. We used the DFTB+ library⁷⁶ with the matsci-0-3 parameters^{77,78} to generate the Hamiltonian and overlap matrices for our calculations. To create the crystal structure for the DFTB+ calculations, we used the Atomic Simulator Environment⁷⁹. All of our calculations were done at the Γ point only.

Algorithm 1 An adaptive implementation of WOM using the second-order Runge-Kutta method.

```

Set  $\delta\beta, \beta_f$  ( $\beta_f$  the target inverse temperature)
Set  $\beta_i = 0$ 
Set tolerance  $\epsilon = 10^{-2}$ 
Set early exit tolerance  $\epsilon_2 = 10^{-4}$ 
Set previous  $\delta\beta$ :  $\delta\beta_p = 0$ 
Set  $H, S, \mu$ 
Set  $\Omega = \Omega_0$ 
while  $\beta_i < \beta_f$  do
  Perform single step of RK1 to get  $\Omega_c$ 
  Perform single step of RK2 to get  $\Omega'$ 
  Calculate  $e_n = \|\Omega' - \Omega_c\|_2$ 
  while  $e_n > \epsilon$  do
     $\delta\beta \leftarrow \delta\beta \sqrt{\frac{\epsilon}{e_n}}$ 
    Perform single step of RK2 to get new  $\Omega'$ 
    Calculate  $e_n = \|\Omega' - \Omega_c\|_2$ 
  end while
  Calculate  $d_n = \|\Omega - \Omega'\|_2$ 
   $\Omega \leftarrow \Omega'$ 
   $\beta_i \leftarrow \beta_i + \delta\beta$ 
   $\delta\beta \leftarrow \delta\beta \sqrt{\frac{\epsilon}{e_n}}$ 
  if  $d_n > \epsilon_2$  then
    break
  end if
end while
End

```

For the grand canonical method, we solve Eqs. (12) and (13) using the average of the highest occupied and lowest unoccupied eigenvalues of H as the value for μ . For the canonical method, we solve Eqs. (20) and (21) while simultaneously solving Eq. (19) to update μ . For both cases, we end at a temperature of 3157 K. Both methods were implemented using an adaptive step⁸⁰ second-order Runge-Kutta method with a tolerance $\epsilon = 10^{-2}$ (Algorithm 1). The code can be found online⁸¹. The eigenvalue spectra of P obtained by these methods for a 250 atom supercell of aluminum are shown in Fig. 1 (absolute errors are plotted in Supplementary Information I). The results of both methods coincide with the exact eigenvalue spectra obtained by solving Eq. (10) or Eq. (14) directly. We also compare electronic energies $E = 2\text{Tr}[S^{-1}PS^{-1}H]$ obtained from our methods to those obtained via direct diagonalization for 16, 54, 128, and 250 atom supercells. For the grand canonical method, we observe that the relative difference is between 0.0008% and 0.0027%. For the canonical method, the relative difference is between 0.0154% and 0.0329%. For increased accuracy, the Runge-Kutta tolerance would need to be tightened and potentially combined with a higher order method. These results demonstrate the effectiveness of our methods in obtaining the Fermi-Dirac density matrices at finite temperatures for a tight-binding Hamiltonian in a non-orthogonal basis.

We also tested how the adaptive step implementations of our method scale with the size of the system. In this work, we consider systems of aluminum with 16, 54, 128, and 250 atoms. The number of evaluations of Eq. (12) or

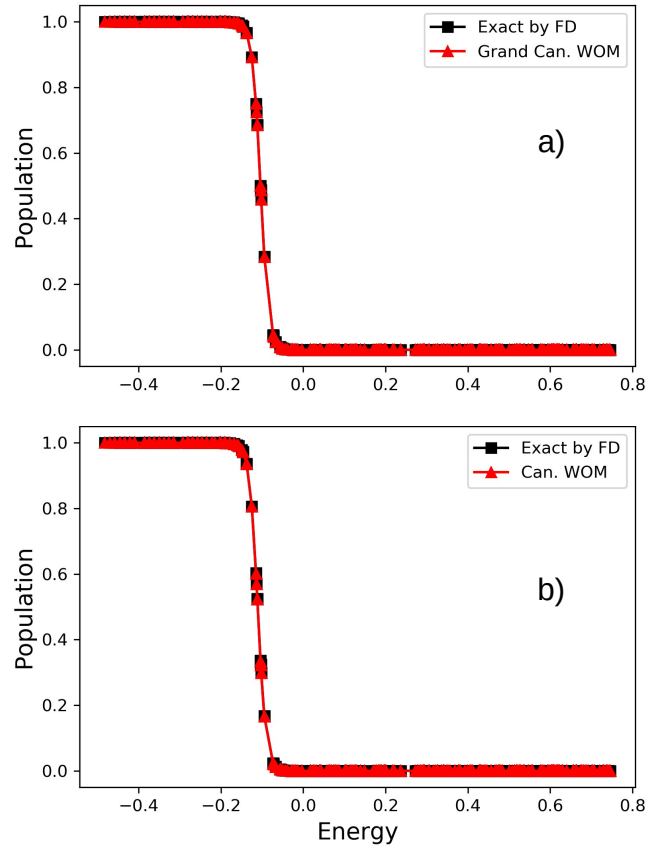


FIG. 1. Eigenvalue spectra of a) the exact matrix obtained by calculating Eq. (10) and the matrix obtained by solving Eqs. (12) and (13); b) the exact matrix obtained by calculating Eq. (14) and the matrix obtained by solving Eqs. (20) and (21) for a tight-binding treatment of aluminum with 250 atoms and 750 electrons. In each case, the spectra of our results demonstrate strong agreement with the exact spectra.

Eq. (18) required for our methods to reach convergence at different temperatures for each system are displayed in Fig. 2. Each evaluation of Eq. (12) requires four matrix multiplications and each evaluation of Eq. (20) requires six matrix multiplications. If $S = 1$, such as when using an initial Cholesky or Löwdin orthogonalization of H , this reduces to three matrix multiplications per evaluation for either equation. These results demonstrate that the number of calculations needed by the adaptive step implementations of our methods grows slowly as the system is increased from 16 to 250 atoms; in Supplementary Information II, we plot the number of multiplications vs. number of atoms (up to 1024) to show how the number of multiplications plateaus. Furthermore, the linear relation between the number of matrix multiplications and a logarithmic scale of the temperature in Fig. 2 indicates that the number of calculations required for convergence decreases exponentially with increasing temperature.

We also wanted to confirm that our canonical method can be used to obtain the correct trend of the specific

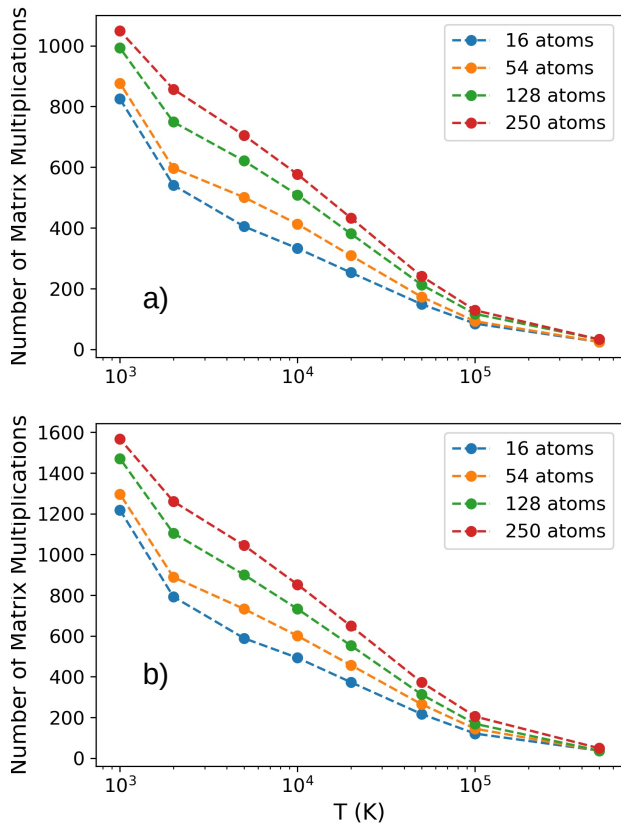


FIG. 2. Number of matrix multiplications required to reach convergence for 16, 54, 128, and 250 atom supercells of aluminum as the temperature is changed when solving a) Eqs. (12) and (13) and b) Eqs. (20) and (21). In each case, we used the adaptive implementation of our methods outlined in Algorithm 1.

heat C_v due to the electrons while solving Eqs. (20) and (21), which can be obtained from

$$C_v = -2k\beta^2 \text{Tr} \left(S^{-1} \frac{d\Omega^\dagger}{d\beta} \Omega A + S^{-1} \Omega^\dagger \frac{d\Omega}{d\beta} A \right). \quad (22)$$

At temperatures much lower than the Fermi temperature, $C_v \sim \gamma T$ where γ is a constant that depends on the material. For metals, the theoretical value γ_{th} can be calculated using the Sommerfeld free electron theory, though there is often a discrepancy between γ_{th} and the value observed in experiments γ_e . The values for aluminum are $\gamma_{th} = 0.912 \text{ mJ/mol/K}^2$ and $\gamma_e = 1.35 \text{ mJ/mol/K}^2$. To calculate the γ obtained using our canonical method, we evaluated Eq. (22) at several temperatures and performed a least squares linear regression to obtain the slope. The data and resulting fit for the 250 atom supercell are plotted in Fig. 3. We see that the fit had $R^2 = 0.99993$ and gave $\gamma = 1.493 \text{ mJ/mol/K}^2$, which is 10.6% larger than γ_e .

As discussed at the beginning of Sec. II, sparsity arises naturally in electronic structure problems because of Kohn's near-sightedness principle and minimization

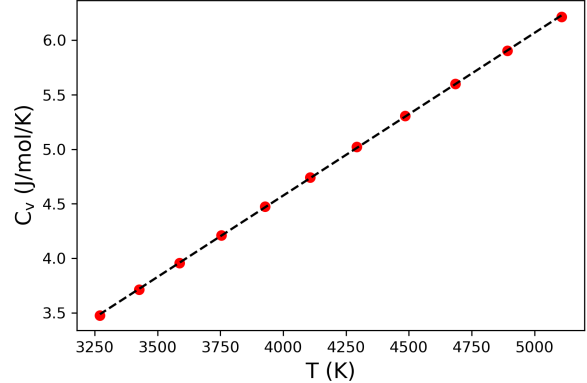


FIG. 3. The dependence of the specific heat C_v on the temperature T for an aluminum system with 250 atoms. The red dots are calculated according to Eq. (22) and the black dashed line indicates the fit using a least squares linear regression.

based approaches to calculating the density matrix take advantage of this to achieve $O(N)$ scaling. Because of this, we wanted to investigate the effect that temperature had on the sparsity of the density matrix. To do so, we implemented the WOM method in the NTPoly library¹⁷. We evolve the Löwdin orthogonalized version of Ω in the grand canonical and canonical ensembles. As a test case, we used the tight-binding Hamiltonian of a bulk silicon system of 6912 atoms generated with the pbc-0-3 parameter set⁸³. During the calculation, NTPoly automatically filters matrix values below some threshold to maintain sparsity. We plot the percentage of non-zero elements vs temperature for threshold choices of 10^{-6} , 10^{-7} , and 10^{-8} in Fig. 4. With the WOM method, fill in of the density matrix occurs gradually as the temperature decreases, ensuring that sparse linear algebra can be used for the whole process. This, combined with the number of multiplications being roughly constant with the system size (Supplementary Information II), means that linear scaling performance can be achieved when the WOM method is used with sufficiently large systems.

A. Comparison with the Fermi Operator Expansion

To further evaluate the WOM method, we compare it to the Fermi Operator Expansion (FOE) method, which expands the Fermi-Dirac distribution using Chebyshev polynomials¹⁸. The FOE method is implemented in the CheSS library¹⁶ and is regularly used in production calculations with the BigDFT code⁸⁴. As a test case, we use a 108 atom supercell of bulk silicon coming from the Siesta code⁸⁵ with a final temperature of 3157K. We computed this system with the PBE functional⁸⁶, the DZP basis set, a mesh cutoff of 300 Ry, an energy shift of 0.01 Ry, and ONCV pseudopotentials⁸⁷ taken from PseudoDojo^{88,89}. The number of matrix multiplications and

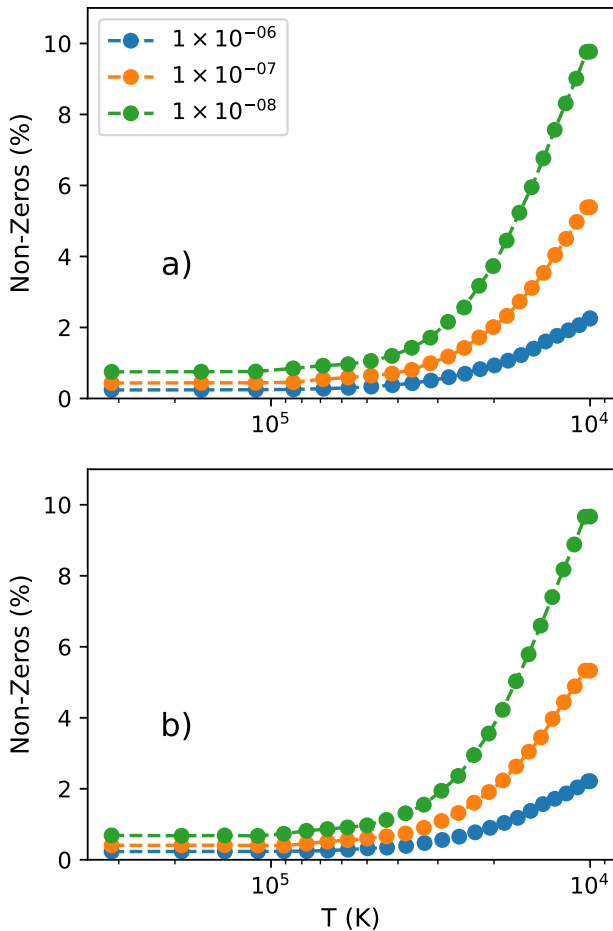


FIG. 4. Sparsity of the density matrix of a 6912 atom supercell of silicon vs temperature. Calculations are performed for the: a) grand canonical and b) canonical ensembles. The legends indicate the threshold used when counting the number of elements in the density matrix that were non-zero.

error in the density matrix using different tolerances for the WOM method and numbers of polynomials for FOE are plotted in Fig. 5. For this test case, we find that WOM and FOE require a similar number of multiplications, depending on the required precision.

There are a number of weaknesses of the FOE method that are addressed by WOM. First, the number of polynomials required depends heavily on the ratio of the HOMO-LUMO gap to the spectral width¹⁶. For this reason, we have chosen a matrix coming from Siesta instead of the earlier tight-binding matrices as a test case. The number of polynomials required would be even larger if, for example, core electrons were included. In contrast to FOE, the ratio of the gap to spectral width only affects the starting temperature (after the first step) of the WOM iterations. In Supplementary Information III, we investigate more closely how the number of iterations is affected by the size of the gap and spectral width. An-

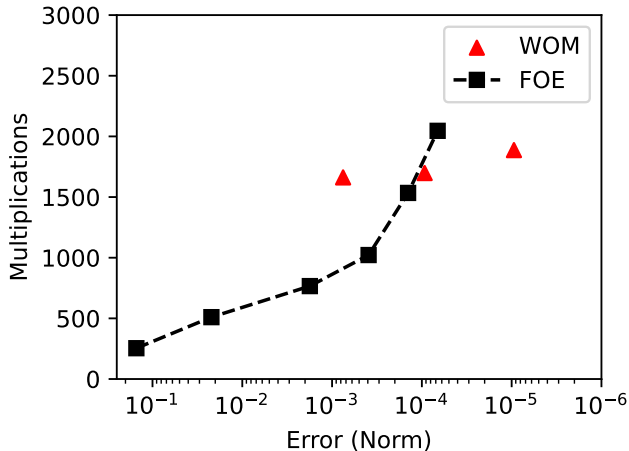


FIG. 5. Number of multiplications required for the WOM and FOE methods to compute a 108 atom silicon system at 3157K in the grand canonical ensemble. WOM calculations were performed with a threshold of 0.1, 0.05, and 0.01. Error is reported as norm of the difference between the density matrix computed with each method and with exact diagonalization. In both cases, we use the Löwdin orthogonalized version of the Hamiltonian.

other drawback to the FOE method is that to compute the chemical potential, one needs to store all intermediate matrix powers in memory, whereas WOM only needs to store a few matrices. Storing intermediate matrices would also be necessary if one wanted to compute the density matrix at different temperatures for properties like the specific heat, which come out automatically with WOM. This characteristic also makes WOM potentially useful when restarting a calculation: the stored wave operator matrix from a previous calculation can be loaded in from disk and iterated to an even lower temperature.

In order to reduce the number of multiplications required for FOE, a variation of the Patterson - Stockmeyer method⁹⁰ was proposed by Liang and coworkers⁹¹. However, this method is challenging to use in practice: there is significant fill in that occurs with intermediate matrices and root finding is needed to get the chemical potential (though some intermediate matrices can be saved). This method has recently been shown to be useful in the dense matrix case using GPUs, where managing sparsity is not an issue⁹². We note as well that evaluations of the Fermi-Operator Expansion frequently target the zero temperature case, where the number of polynomials can be reduced by expanding the complementary error functions instead of the true Fermi-Dirac distribution or by using the Jackson approximation⁹³. For the zero temperature case, these modifications may be used to help the FOE method significantly outperform WOM (see Supplementary Information III for more discussion of the zero temperature case).

VI. CONCLUSION

We have developed positivity-preserving methods for calculating the Fermi-Dirac density matrices at finite temperatures for both the grand canonical (Sec. III) and canonical (Sec. IV) ensembles. These methods are based on minimization of the square root of the density matrix (Ω) and the modelling of a physical process of cooling a state initially at infinite temperature down to the temperature of interest. The effectiveness of WOM is demonstrated by considering tight-binding models of aluminum and silicon of various system sizes. Additionally, the number of steps required to reach convergence is shown to be independent of the number of atoms in the system. To the best of our knowledge, this work is the first to make use of Ω as a computational tool. This approach may lay the groundwork for a new generation of methods that utilize Ω for solving electronic structure problems. To facilitate this, we made the code publicly available on GitHub⁸¹. For a practical implementation in Density Functional Theory codes, using minimization as a replacement for the self-consistent cycle could be used to further reduce the computational cost^{48,94}. A possible future direction is to utilize the fact that a low-temperature Fermi-Dirac density matrix is of a low rank, hence it is possible to further accelerate calculations by utilizing low-rank corner space techniques recently developed for solving master equations for large open quantum systems^{95–99}.

ACKNOWLEDGMENTS

The authors are grateful to George Booth for helping with the PySCF library¹⁰⁰ and valuable discussions. J.M.L. was supported by the Louisiana Board of Regents' Graduate Fellowship Program. D.I.B. is supported by the Army Research Office (ARO) (grant W911NF-23-1-0288; program manager Dr. James Joseph), Air Force Office of Scientific Research (AFOSR) Young Investigator Research Program (grant FA9550-16-1-0254; program manager Dr. Fariba Fahroo), and the Alexander von Humboldt Foundation (Humboldt Research Fellowship for Experienced Researchers).

CONFLICT OF INTEREST

The authors have no conflicts to disclose.

DATA AVAILABILITY STATEMENT

Implementations of the described algorithms are publicly available on GitHub⁸¹. An implementation of the described algorithms is also available as part of NT-Poly¹⁰¹. The remaining data that support the findings

of this study are available from the corresponding author upon reasonable request.

Appendix A: Non-Orthonormal Fermi-Dirac

We want to derive an expression for the Fermi-Dirac distribution that is valid for a general, non-orthonormal basis. Consider the general, non-orthonormal basis set: $\{|i\rangle\}_{i=0}^N$ where N is the dimension of the system in question. Let $S = (\langle i|j\rangle)$ be the overlap matrix, \hat{H} be the Hamiltonian operator, and $\hat{\rho}$ be the Fermi-Dirac distribution

$$\hat{\rho}(\beta) = \frac{\hat{I}}{\hat{I} + \exp[\beta(\hat{H} - \mu\hat{I})]}. \quad (\text{A1})$$

Now let $P = (\langle i|\hat{\rho}|j\rangle)$ and $H = (\langle i|\hat{H}|j\rangle)$ be the representations of $\hat{\rho}$ and \hat{H} in the non-orthonormal basis, respectively. The Taylor series expansion for $\hat{\rho}$ reads

$$P = \sum_{n=0}^{\infty} a_n \langle i|\hat{A}^n|j\rangle, \quad (\text{A2})$$

where $\hat{A} = (\hat{H} - \mu)$ and has the representation $A = (\langle i|\hat{A}|j\rangle)$ in the non-orthonormal basis. The goal is to find the representation of $\langle i|\hat{A}^n|j\rangle$ in the non-orthonormal basis so that we can obtain a concise expression for P . We start by considering how \hat{A} acts on a basis vector $|j\rangle$. If we expand $|j\rangle$ in the basis $\{|k\rangle\}$, we get

$$\langle i|\hat{A}|j\rangle = \langle i|\sum_k C_{kj}|k\rangle = \sum_k C_{kj} \langle i|k\rangle = SC \quad (\text{A3})$$

where $C = S^{-1}A$ is just the matrix of coefficients obtained from $\hat{A}|j\rangle$. We can perform similar expansions to obtain $\langle i|\hat{A}^n|j\rangle$ for $n > 1$ and then use induction to show that

$$\langle i|\hat{A}^n|j\rangle = A(S^{-1}A)^{n-1}. \quad (\text{A4})$$

If we multiply both sides of Eq. (A2) by S^{-1} on the left and substitute in for $\langle i|\hat{A}^n|j\rangle$, we obtain

$$S^{-1}P = \sum_{n=0}^{\infty} a_n (S^{-1}A)^n = [I + \exp[\beta S^{-1}A]]^{-1}. \quad (\text{A5})$$

Finally, we replace A with $\langle i|(\hat{H} - \mu I)|j\rangle$ and solve for P to obtain

$$P = S [I + \exp[\beta(S^{-1}H - \mu I)]]^{-1}. \quad (\text{A6})$$

Note that P is the real density matrix in the non-orthogonal basis. Electronic structure codes frequently make use of the density kernel K , which is the representation of the density matrix in the dual basis^{102,103}. The density kernel can be obtained by

$$K = S^{-1}PS^{-1}, \quad (\text{A7})$$

which is the transformation of P to the dual basis.

Appendix B: The root of P

We want to derive Eq. (11). To simplify matters, we introduce the following

$$f(x) = [1 + e^x]^{-1/2}, \quad (\text{B1})$$

$$A = S^{-1}H - \mu I, \quad (\text{B2})$$

so that Eq. (11) can be written as

$$P(\beta) = Sf(\beta A)f(\beta A), \quad (\text{B3})$$

$$\Omega(\beta) = S^{1/2}f(\beta A). \quad (\text{B4})$$

Now consider expressing $\Omega^\dagger\Omega = \Omega(\beta)^\dagger\Omega(\beta)$ in terms of the Maclaurin series expansion of $f(\beta A)$, which yields

$$\Omega^\dagger\Omega = f(\beta A^\dagger)Sf(\beta A), \quad (\text{B5})$$

$$= \sum_{i,j=0}^{\infty} \frac{f^{(i)}(0)}{i!} (A^\dagger)^i \beta^i S \frac{f^{(j)}(0)}{j!} A^j \beta^j. \quad (\text{B6})$$

Grouping by powers of β gives

$$\Omega^\dagger\Omega = \sum_{k=0}^{\infty} \sum_{m=0}^k \frac{f^{(m)}(0)f^{(k-m)}(0)}{m!(k-m)!} (A^\dagger)^l S A^{k-m} \beta^k. \quad (\text{B7})$$

It follows from Eq. (B2) that $SA = (SA)^\dagger = A^\dagger S$, which can be used with the fact that $\binom{k}{m} = \frac{k!}{(k-m)!m!}$ to obtain

$$\Omega^\dagger\Omega = \sum_{k=0}^{\infty} \frac{1}{k!} \sum_{m=0}^k \binom{k}{m} f^{(m)}(0)f^{(k-m)}(0) S A^k \beta^k. \quad (\text{B8})$$

Note now that

$$(f(\beta A)f(\beta A))^{(k)}|_{\beta=0} = \sum_{m=0}^k \binom{k}{m} f^{(m)}(0)f^{(k-m)}(0) A^k, \quad (\text{B9})$$

which can be substituted into Eq. (B8) to obtain

$$\Omega^\dagger\Omega = \sum_{k=0}^{\infty} \frac{1}{k!} S [f(\beta A)f(\beta A)]^{(k)}|_{\beta=0} \beta^k, \quad (\text{B10})$$

$$= \sum_{k=0}^{\infty} \frac{1}{k!} P^{(k)}(0) \beta^k, \quad (\text{B11})$$

$$= P(\beta). \quad (\text{B12})$$

¹A. V. Akimov and O. V. Prezhdo, *Chemical Reviews* **115**, 5797 (2015).

²S. Goedecker, *Rev. Mod. Phys.* **71**, 1085 (1999).

³D. R. Bowler and T. Miyazaki, *Reports on Progress in Physics* **75**, 036503 (2012).

⁴L. E. Ratcliff, S. Mohr, G. Huhs, T. Deutsch, M. Masella, and L. Genovese, *Wiley Interdiscip. Rev.: Comput. Mol. Sci.* **7**, e1290 (2017).

⁵W. Dawson, A. Degomme, M. Stella, T. Nakajima, L. E. Ratcliff, and L. Genovese, *WIREs Computational Molecular Science* **12**, e1574 (2022).

⁶M. J. Cawkwell and A. M. N. Niklasson, *J. Chem. Phys.* **137**, 134105 (2012).

⁷R. Schade, T. Kenter, H. Elgabarty, M. Lass, O. Schütt, A. Lazzaro, H. Pabst, S. Mohr, J. Hutter, T. D. Kühne, and C. Plessl, *Parallel Computing* **111**, 102920 (2022).

⁸A. M. N. Niklasson, *The Journal of Chemical Physics* **147**, 054103 (2017).

⁹C. F. A. Negre, M. E. Wall, and A. M. N. Niklasson, *The Journal of Chemical Physics* **158**, 074108 (2023).

¹⁰U. Borštnik, J. VandeVondele, V. Weber, and J. Hutter, *Parallel Computing* **40**, 47 (2014).

¹¹L. Lin, C. Yang, J. Lu, L. Ying, and W. E, *SIAM Journal on Scientific Computing* **33**, 1329 (2011).

¹²L. Lin, C. Yang, J. C. Meza, J. Lu, L. Ying, and W. E, *ACM Transactions on Mathematical Software* **37**, 1 (2011).

¹³M. Jacquelin, L. Lin, and C. Yang, *ACM Transactions on Mathematical Software* **43**, 1 (2017).

¹⁴E. H. Rubensson, E. Rudberg, A. Kruchinina, and A. G. Artemov, *SoftwareX* **19**, 101159 (2022).

¹⁵N. Bock, C. F. A. Negre, S. M. Mniszewski, J. Mohd-Yusof, B. Aradi, J.-L. Fattebert, D. Osei-Kuffuor, T. C. Germann, and A. M. N. Niklasson, *The Journal of Supercomputing* **74**, 6201 (2018).

¹⁶S. Mohr, W. Dawson, M. Wagner, D. Caliste, T. Nakajima, and L. Genovese, *Journal of Chemical Theory and Computation* **13**, 4684 (2017).

¹⁷W. Dawson and T. Nakajima, *Computer Physics Communications* **225**, 154 (2018).

¹⁸S. Goedecker and M. Teter, *Phys. Rev. B* **51**, 9455 (1995).

¹⁹A. M. N. Niklasson, *Phys. Rev. B* **68**, 233104 (2003).

²⁰A. M. N. Niklasson, *The Journal of Chemical Physics* **129**, 244107 (2008).

²¹P. P. Pratapa, P. Suryanarayana, and J. E. Pask, *Computer Physics Communications* **200**, 96 (2016).

²²J. Aarons, M. Sarwar, D. Thompsett, and C.-K. Skylaris, *The Journal of Chemical Physics* **145**, 220901 (2016).

²³S. M. Mniszewski, R. Perriot, E. H. Rubensson, C. F. A. Negre, M. J. Cawkwell, and A. M. N. Niklasson, *J. Chem. Theory Comput.*, 11 (2019).

²⁴J. Aarons and C.-K. Skylaris, *The Journal of Chemical Physics* **148**, 074107 (2018), publisher: American Institute of Physics.

²⁵Y. Cytter, E. Rabani, D. Neuhauser, and R. Baer, *Phys. Rev. B* **97**, 115207 (2018).

²⁶R. Baer, D. Neuhauser, and E. Rabani, *Annual Review of Physical Chemistry* **73**, 255 (2022).

²⁷N. D. Mermin, *Phys. Rev.* **137**, A1441 (1965).

²⁸E. K. U. Gross, L. N. Oliveira, and W. Kohn, *Physical Review A* **37**, 2809 (1988).

²⁹L. N. Oliveira, E. K. U. Gross, and W. Kohn, *Phys. Rev. A* **37**, 2821 (1988).

³⁰A. Pribram-Jones, S. Pittalis, E. K. U. Gross, and K. Burke, in *Frontiers and Challenges in Warm Dense Matter*, edited by F. Graziani, M. P. Desjarlais, R. Redmer, and S. B. Trickey (Springer International Publishing, Cham, 2014) pp. 25–60.

³¹J.-D. Chai, *The Journal of Chemical Physics* **136**, 154104 (2012).

³²S. Grimme and A. Hansen, *Angewandte Chemie International Edition* **54**, 12308 (2015).

³³M. Filatov, *WIREs Computational Molecular Science* **5**, 146 (2015).

³⁴A. D. Rabuck and G. E. Scuseria, *The Journal of Chemical Physics* **110**, 695 (1999).

³⁵M. S. Daw, *Physical Review B* **47**, 10895 (1993), publisher: American Physical Society.

³⁶M. Challacombe, *The Journal of Chemical Physics* **110**, 2332 (1999).

³⁷X.-P. Li, R. W. Nunes, and D. Vanderbilt, *Physical Review B*

- 47, 10891 (1993), publisher: American Physical Society.
- ³⁸R. Lai and J. Lu, *Journal of Computational Physics* **315**, 194 (2016).
- ³⁹R. Lai, J. Lu, and S. Osher, *Communications in Mathematical Sciences* **13**, 2097 (2015).
- ⁴⁰M. Arita, D. R. Bowler, and T. Miyazaki, *Journal of Chemical Theory and Computation* **10**, 5419 (2014).
- ⁴¹A. D. Daniels, J. M. Millam, and G. E. Scuseria, *The Journal of Chemical Physics* **107**, 425 (1997).
- ⁴²J. M. Millam and G. E. Scuseria, *The Journal of Chemical Physics* **106**, 5569 (1997).
- ⁴³D. R. Bowler and M. J. Gillan, *Computer Physics Communications* **120**, 95 (1999).
- ⁴⁴M. Challacombe, *The Journal of Chemical Physics* **110**, 2332 (1999).
- ⁴⁵Y. Shao, C. Saravanan, M. Head-Gordon, and C. A. White, *The Journal of Chemical Physics* **118**, 6144 (2003).
- ⁴⁶T. Helgaker, H. Larsen, J. Olsen, and P. Jørgensen, *Chemical Physics Letters* **327**, 397 (2000).
- ⁴⁷H. Larsen, J. Olsen, P. Jørgensen, and T. Helgaker, *The Journal of Chemical Physics* **115**, 9685 (2001).
- ⁴⁸P. Salek, S. Høst, L. Thøgersen, P. Jørgensen, P. Manninen, J. Olsen, B. Jansík, S. Reine, F. Pawłowski, E. Tellgren, T. Helgaker, and S. Coriani, *The Journal of Chemical Physics* **126**, 114110 (2007).
- ⁴⁹R. W. Nunes and D. Vanderbilt, *Physical Review B* **50**, 17611 (1994).
- ⁵⁰E. Hernández, M. J. Gillan, and C. M. Goringe, *Physical Review B* **53**, 7147 (1996).
- ⁵¹A. Uhlmann, *Rep. Math. Phys.* **24**, 229 (1986).
- ⁵²J. J. Włodarz, *J. Chem. Phys.* **100**, 7476 (1994).
- ⁵³B. Reznik, *Physical Review Letters* **76**, 1192 (1996).
- ⁵⁴S. Gheorghiu-Svirshevski, *Physical Review A* **63**, 022105 (2001).
- ⁵⁵G. P. Beretta, *Modern Physics Letters A* **20**, 977 (2005).
- ⁵⁶G. P. Beretta, *Physical Review E* **73**, 026113 (2006).
- ⁵⁷A. Yahalom and R. Engelman, *Physica A* **371**, 368 (2006).
- ⁵⁸C. Tronci, *J. Geom. Mech* **11**, 639 (2019).
- ⁵⁹G. McCaul, D. V. Zhdanov, and D. I. Bondar, arXiv:2302.13208 (2023).
- ⁶⁰L. Joubert-Doriol, I. G. Ryabinkin, and A. F. Izmaylov, *J. Chem. Phys.* **141**, 234112 (2014).
- ⁶¹M. Levy, J. P. Perdew, and V. Sahni, *Physical Review A* **30**, 2745 (1984).
- ⁶²M. Levy and Hui Ou-Yang, *Physical Review A* **38**, 625 (1988), publisher: American Physical Society.
- ⁶³J. A. Flores and J. Keller, *Physical Review A* **45**, 6259 (1992), publisher: American Physical Society.
- ⁶⁴W. Kohn, *Phys. Rev. Lett.* **76**, 3168 (1996).
- ⁶⁵E. Prodan and W. Kohn, *Proceedings of the National Academy of Sciences* **102**, 11635 (2005).
- ⁶⁶F. Bloch, *Zeitschrift für Physik* **74**, 295 (1932).
- ⁶⁷R. A. Horn and C. R. Johnson, *Matrix Analysis*, 2nd ed. (Cambridge Univ. Press, 32 Avenue of the Americas, New York, NY 10013-2473, USA, 2013).
- ⁶⁸R. McWeeny, *Reviews of Modern Physics* **32**, 335 (1960).
- ⁶⁹A. H. R. Palser and D. E. Manolopoulos, *Physical Review B* **58**, 12704 (1998), publisher: American Physical Society.
- ⁷⁰S. Y. Qiu, C. Z. Wang, K. M. Ho, and C. T. Chan, *Journal of Physics: Condensed Matter* **6**, 9153 (1994).
- ⁷¹J. C. Slater and G. F. Koster, *Physical Review* **94**, 1498 (1954).
- ⁷²M. M. Maslov, A. I. Podlivaev, and K. P. Katin, *Molecular Simulation* **42**, 305 (2016), publisher: Taylor & Francis.
- ⁷³G.-B. Liu, W.-Y. Shan, Y. Yao, W. Yao, and D. Xiao, *Physical Review B* **88**, 085433 (2013), publisher: American Physical Society.
- ⁷⁴F.-C. Chuang, C. Z. Wang, and K. H. Ho, *Physical Review B* **73**, 125431 (2006), publisher: American Physical Society.
- ⁷⁵G. Staszewska, P. Staszewski, N. E. Schultz, and D. G. Truhlar, *Physical Review B* **71**, 045423 (2005), publisher: American Physical Society.
- ⁷⁶B. Hourahine, B. Aradi, V. Blum, F. Bonafé, A. Buccheri, C. Camacho, C. Cevallos, M. Y. Deshayé, T. Dumitrică, A. Dominguez, S. Ehlert, M. Elstner, T. van der Heide, J. Hermann, S. Irle, J. J. Kranz, C. Köhler, T. Kowalczyk, T. Kubař, I. S. Lee, V. Lutsker, R. J. Maurer, S. K. Min, I. Mitchell, C. Negre, T. A. Niehaus, A. M. N. Niklasson, A. J. Page, A. Pecchia, G. Penazzi, M. P. Persson, J. Řezáč, C. G. Sánchez, M. Sternberg, M. Stöhr, F. Stuckenberg, A. Tkatchenko, V. W.-z. Yu, and T. Frauenheim, *J. Chem. Phys.* **152**, 124101 (2020).
- ⁷⁷J. Frenzel, A. F. Oliveira, H. A. Duarte, T. Heine, and G. Seifert, *Zeitschrift für anorganische und allgemeine Chemie* **631**, 1267 (2005).
- ⁷⁸H. Manzano, A. N. Enyashin, J. S. Dolado, A. Ayuela, J. Frenzel, and G. Seifert, *Advanced Materials* **24**, 3239 (2012).
- ⁷⁹A. H. Larsen, J. J. Mortensen, J. Blomqvist, I. E. Castelli, R. Christensen, M. Dułak, J. Friis, M. N. Groves, B. Hammer, C. Hargus, E. D. Hermes, P. C. Jennings, P. B. Jensen, J. Kermode, J. R. Kitchin, E. L. Kolsbjerg, J. Kubal, K. Kaasbjerg, S. Lysgaard, J. B. Maronsson, T. Maxson, T. Olsen, L. Pastewka, A. Peterson, C. Rostgaard, J. Schiøtz, O. Schütt, M. Strange, K. S. Thygesen, T. Vegge, L. Vilhelmsen, M. Walter, Z. Zeng, and K. W. Jacobsen, *J. Phys.: Condens. Matter* **29**, 273002 (2017).
- ⁸⁰G. Söderlind and L. Wang, *Journal of Computational and Applied Mathematics* **185**, 225 (2006).
- ⁸¹J. M. Leamer, “Dmm,” <https://github.com/jleamer/DMM> (2020).
- ⁸²C. Kittel, *Introduction to Solid State Physics*, 8th ed. (John Wiley and Sons, Inc., 111 River St., Hoboken, NJ 07030-5774, USA, 2005).
- ⁸³A. Sieck, Paderborn University thesis (2000).
- ⁸⁴L. E. Ratcliff, W. Dawson, G. Fiscaro, D. Caliste, S. Mohr, A. Degomme, B. Videau, V. Cristiglio, M. Stella, M. D’Alessandro, S. Goedecker, T. Nakajima, T. Deutsch, and L. Genovese, *The Journal of Chemical Physics* **152**, 194110 (2020).
- ⁸⁵A. García, N. Papior, A. Akhtar, E. Artacho, V. Blum, E. Bosoni, P. Brandimarte, M. Brandbyge, J. I. Cerdá, F. Corsetti, R. Cuadrado, V. Dikan, J. Ferrer, J. Gale, P. García-Fernández, V. M. García-Suárez, S. García, G. Huhs, S. Illera, R. Korytár, P. Koval, I. Lebedeva, L. Lin, P. López-Tarifa, S. G. Mayo, S. Mohr, P. Ordejón, A. Postnikov, Y. Pouillon, M. Pruneda, R. Robles, D. Sánchez-Portal, J. M. Soler, R. Ullah, V. W.-z. Yu, and J. Junquera, *The Journal of Chemical Physics* **152**, 204108 (2020).
- ⁸⁶J. P. Perdew, K. Burke, and M. Ernzerhof, *Physical Review Letters* **77**, 3865 (1996).
- ⁸⁷D. R. Hamann, *Physical Review B* **88**, 085117 (2013).
- ⁸⁸M. J. van Setten, M. Giantomassi, E. Bousquet, M. J. Verstraete, D. R. Hamann, X. Gonze, and G.-M. Rignanese, *Computer Physics Communications* **226**, 39 (2018).
- ⁸⁹A. García, M. J. Verstraete, Y. Pouillon, and J. Junquera, *Computer Physics Communications* **227**, 51 (2018).
- ⁹⁰M. S. Paterson and L. J. Stockmeyer, *SIAM Journal on Computing* **2**, 60 (1973).
- ⁹¹W. Liang, C. Saravanan, Y. Shao, R. Baer, A. T. Bell, and M. Head-Gordon, *The Journal of Chemical Physics* **119**, 4117 (2003).
- ⁹²J. Finkelstein, C. F. A. Negre, and J.-L. Fattebert, *The Journal of Chemical Physics* **159**, 101101 (2023).
- ⁹³L. O. Jay, H. Kim, Y. Saad, and J. R. Chelikowsky, *Computer Physics Communications* **118**, 21 (1999).
- ⁹⁴C. Flamant, G. Kolesov, E. Manousakis, and E. Kaxiras, *Journal of Chemical Theory and Computation* **15**, 6036 (2019).
- ⁹⁵C. Le Bris and P. Rouchon, *Physical Review A* **87**, 022125 (2013).
- ⁹⁶S. Finazzi, A. Le Boité, F. Storme, A. Baksic, and C. Ciuti, *Physical Review Letters* **115**, 080604 (2015).
- ⁹⁷G. McCaul, K. Jacobs, and D. I. Bondar, *Physical Review*

- Research **3**, 013017 (2021).
- ⁹⁸Y.-T. Chen, C. Farquhar, and R. M. Parrish, *npj Quantum Information* **7**, 61 (2021).
- ⁹⁹K. Donatella, Z. Denis, A. Le Boité, and C. Ciuti, *Physical Review A* **104**, 062407 (2021).
- ¹⁰⁰Q. Sun, T. C. Berkelbach, N. S. Blunt, G. H. Booth, S. Guo, Z. Li, J. Liu, J. D. McClain, E. R. Sayfutyarova, S. Sharma, S. Wouters, and G. K. Chan, “Pyscf: the python-based simulations of chemistry framework,” (2017), <https://onlinelibrary.wiley.com/doi/pdf/10.1002/wcms.1340>.
- ¹⁰¹W. Dawson, “Ntpoly,” <https://github.com/william-dawson/NTPoly> (2023).
- ¹⁰²S. Mohr, L. E. Ratcliff, P. Boulanger, L. Genovese, D. Caliste, T. Deutsch, and S. Goedecker, *The Journal of Chemical Physics* **140**, 204110 (2014).
- ¹⁰³P. D. Haynes, C.-K. Skylaris, A. A. Mostofi, and M. C. Payne, *J. Phys.: Condens. Matter* **20**, 294207 (2008).

Supplementary Information - Positivity Preserving Density Matrix Minimization at Finite Temperatures via Square Root

Jacob Leamer and Denys I. Bondar

*Department of Physics and Engineering Physics, Tulane University,
6823 St. Charles Ave., New Orleans, LA 70118, USA*

William Dawson

RIKEN Center for Computational Science, Kobe, Hyogo, 650-0047, Japan.

arXiv:2103.07078v3 [quant-ph] 6 Dec 2023

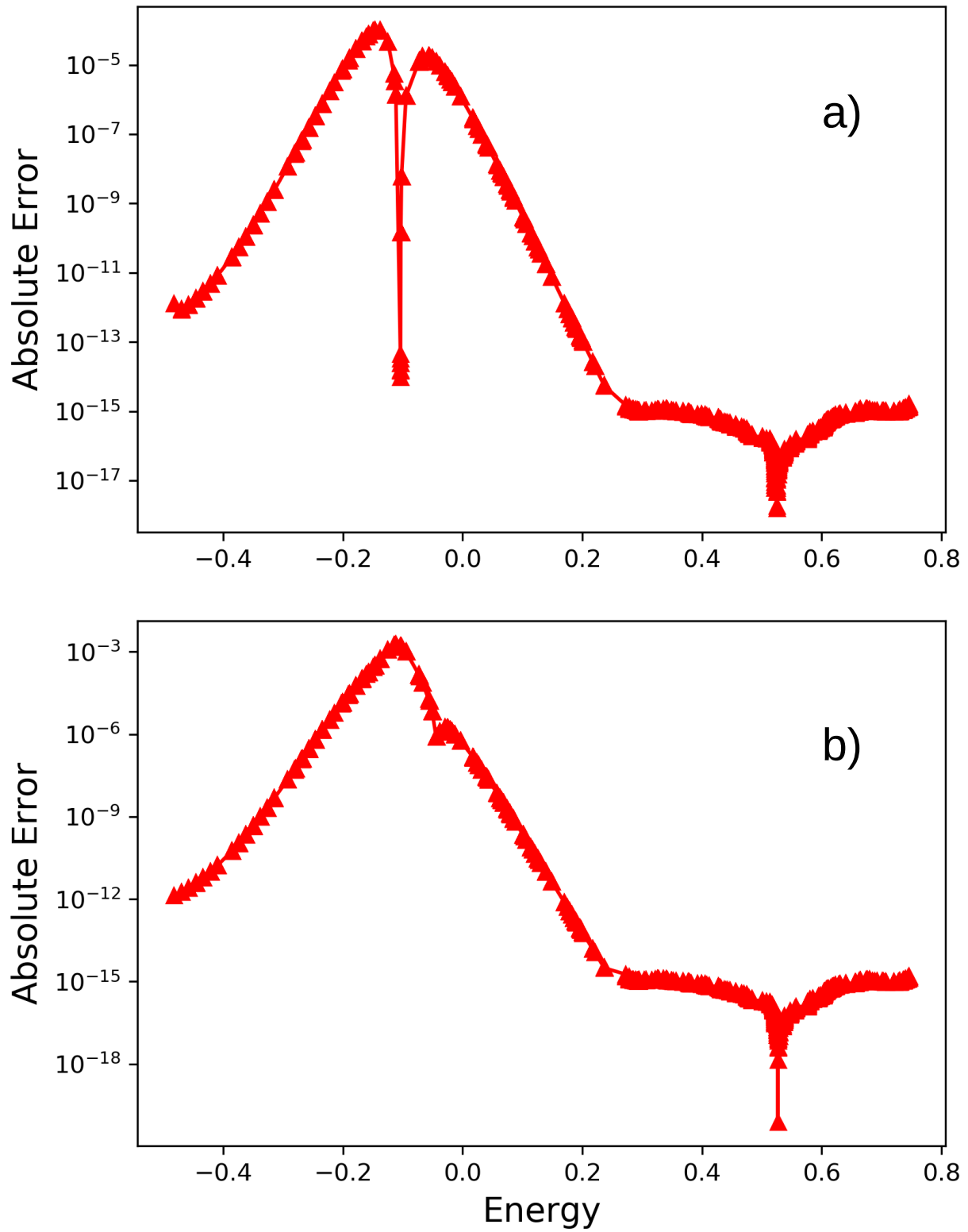


FIG. 1. Absolute error in the occupation numbers between the results obtained by WOM and exact diagonalization for the a) grand canonical and b) canonical ensembles.

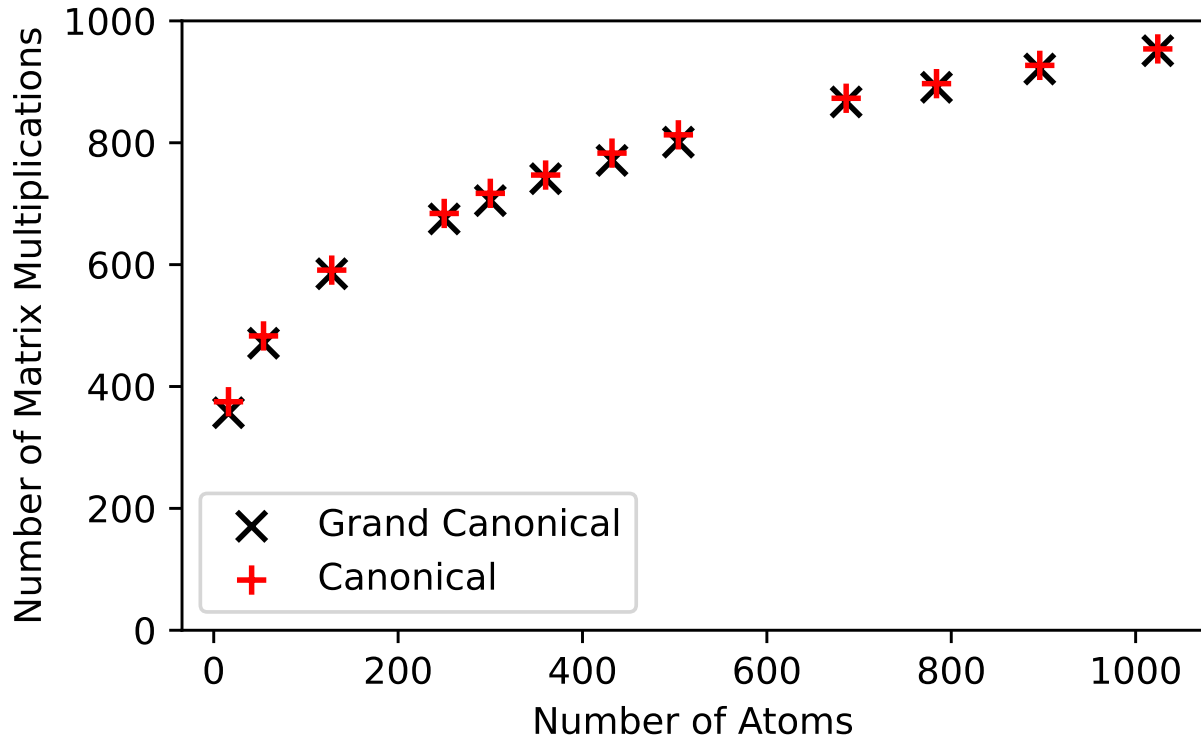


FIG. 2. Number of multiplications required to reach 3157K in the grand canonical and canonicals.

I. ERROR IN OCCUPATION

The error in the occupation numbers of the resulting density matrices obtained by WOM vs. diagonalization for the 250 atom aluminum tight binding system is plotted in Fig. 1. The error is largest near the Fermi level; however, the errors are sufficiently low for practical calculations.

II. MULTIPLICATIONS VS. SYSTEM SIZE

We examined how the number of multiplications grows with the number of atoms using the aluminum tight binding systems as an example (Fig. 2). For this analysis, we use the Löwdin orthogonalized Hamiltonian for computational efficiency. We find that the number of multiplications initially grows with the system size, before finally saturating.

III. IMPACT OF THE HOMO-LUMO GAP

In order to understand the impact of the size of the HOMO-LUMO gap on the convergence of the WOM method, we used the tight-binding model of silicon (108 atoms) and artificially modified the gap by shifting the occupied and virtual orbitals towards / away from the chemical potential. In Fig. 3, we plot the number of multiplications vs. temperature and the errors in occupancy achieved with the Grand Canonical Ensemble version of WOM using several different values for the HOMO-LUMO gap. We find that the number of iterations and error is fairly insensitive to the gap. One significant difference comes from changes in the spectral width (from shifting the eigenvalues outward), which changes the initial temperature after the first step. Additionally, when a low temperature solution is sought, iterations can exit early for systems with a larger gap. This is because the difference in the wave operator at a lower temperature is close to the ground state, which triggers the early exit condition of Algorithm 1. From this data, we conclude that WOM can be applied to both insulating and metallic systems without any changes.

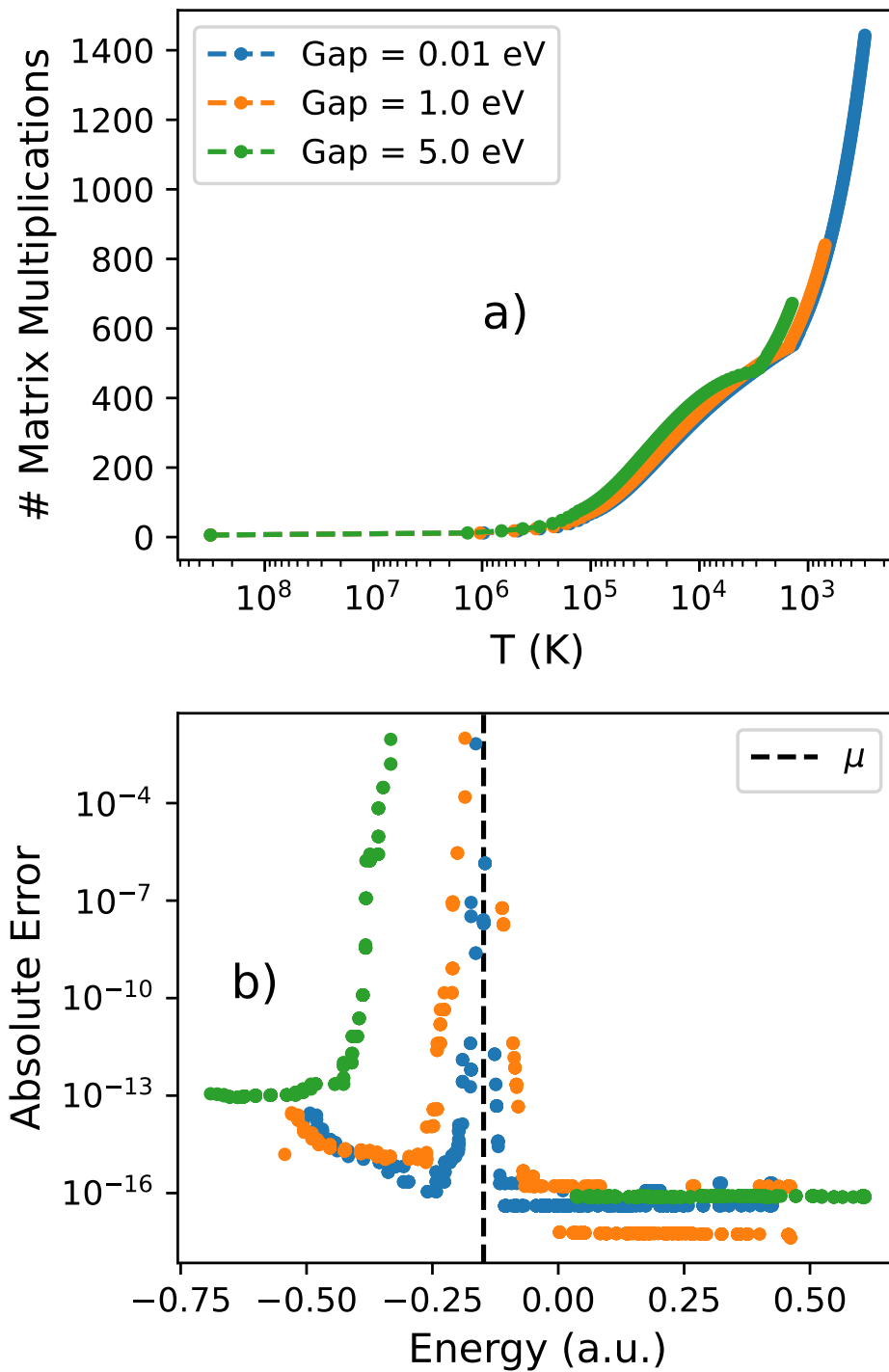


FIG. 3. The effect of the size of the gap on the WOM method. a) The number of matrix multiplications vs. temperature. b) Absolute error in the occupancy vs. orbital energy. Calculations are performed with the Löwdin orthogonalized Hamiltonian with a target temperature of 300K.